Thermal geological model of the city of Guayaquil, Ecuador

Guillermo Soriano [a,*], Tania Espinoza [a,b], Ruben Villanueva [a,b], Inmaculada Gonzalez [b], Andres Montero [b,e], Mauricio Cornejo [c], Katthy Lopez [d]

[a] Escuela Superior Politécnica del Litoral, ESPOL, Centro de Energias Renovables y Alternativas (CERA), Campus Gustavo Galindo Km 30.5 Vía Perimetral, P.O. Box 09-01-5863, Guayaquil, Ecuador
[b] Instituto Nacional de Eficiencia Energetica y Energias Renovables (INER), Av. 6 de Diciembre N33-32 e Ignacio Bossano, Quito, Ecuador
[c] Escuela Superior Politécnica del Litoral, ESPOL, Centro de Nanotecnologia (CIDNA), Campus Gustavo Galindo Km 30.5 Vía Perimetral, P.O. Box 09-01-5863, Guayaquil, Ecuador
[d] Facultad de Ciencias Naturales, Universidad de Guayaquil, Av. Raúl Gómez Lince s/n y Av. Juan Tanca Marengo, Guayaquil, Ecuador
[e] Universidad Regional Amazónica IKIAM, km 7 vía Muyuna, Tena, Ecuador

ARTICLE INFO

ABSTRACT

A thermal-geological model of the city of Guayaquil, Ecuador is presented, by thorough drill core studies and thermal response tests (TRTs) at ten representative locations. The aim of the project was to complete an analysis of the geological and thermal properties to define their suitability for ground source based heating ventilating and air conditioning (HVAC) systems. The first task consisted of performing mineralogical and geotechnical analysis of the samples using X-ray diffraction, optical microscopy, and grain size analysis tests to identify the litho-stratigraphy of ten points or areas in the city of Guayaquil. Simultaneously, field thermal response tests were completed to collect data on thermal properties of the soil in the ten locations. The geological and thermal response test results were used to develop representations of the city lithography as well as its thermal conductivity, resistivity, and undisturbed ground temperature results. These maps constitute a tool to design geothermal cooling systems and define the suitability of using the soil as a heat sink for cooling systems.

© 2016 Elsevier Ltd. All rights reserved.

1. Introduction

A current problem for large cities with tropical climates is the large energy demand generated by mechanical cooling systems in buildings (Lu et al., 2013; Aldossary et al., 2014). In Malaysia, for example, building annual energy consumption is approximately 6090 GWh where 57% of which is due to air conditioning systems (Yau and Hasbi, 2013). In 2006, air conditioning and refrigeration accounted for 33% of electricity consumption in Hong Kong (Fong et al., 2010). The Gulf States (Bahrain, southern Iraq, Kuwait, Oman, Qatar, eastern Saudi Arabia and the United Arab Emirates) consume more than 70% of their energy production on air conditioning systems (El-Dessouky et al., 2004). A number of possible approaches to solving this problem have recently been discussed such as solar cooling systems (Anand et al., 2014; Chan et al., 2010), thermal storage materials (Pintaldi et al., 2015), passive solar cooling via evaporative effects (Best and Rivera, 2015; Chan et al., 2010), hybrid solar thermo-mechanical cooling with conventional cooling systems (Zeyghami et al., 2015), and geothermal-based

cooling systems (GBCSs) (Florides and Kalogirou, 2007; Tsai et al., 2014; Ruiz-Calvo and Montagud, 2014; Kharseh et al., 2015). In the case of Guayaquil, Ecuador, a city with a tropical wet climate (average annual temperature is around 27 °C and average annual relative humidity is around 77% (INAMHI, 2015) with little variation through the year) and close to one of the largest estuarine systems in Latin America, i.e. the Guayaquil Gulf, the application of geothermal-based cooling systems is promising. The implementation of GBCSs requires knowledge of the thermal properties of the ground obtained by thermal response tests (TRTs) (Banjac et al., 2012; Shim and Park, 2013; Boukili Hacene et al., 2012; Esen and Inalli, 2009; Sharqawy et al., 2009; Sanner et al., 2003).

As GBCSs are used to exchange heat with the soil, its technical characteristics such as mineral composition, moisture content, particle size analysis, bulk density, and Atterberg limits can be related to its thermal performance. Previous studies had proposed thermal conductivity predictive models based on mineral composition, bulk density and water content (De Vries, 1963; Johansen, 1977; Kasubuchi, 1984). However, few studies reported the relationship between soil characteristics and its thermal properties. In this sense, Abu-Hamdeh et al. (2001) performed a comparison of two methods in order to evaluate thermal conductivity for four types of soils (sand, sandy loam, loam and clay loam). The authors
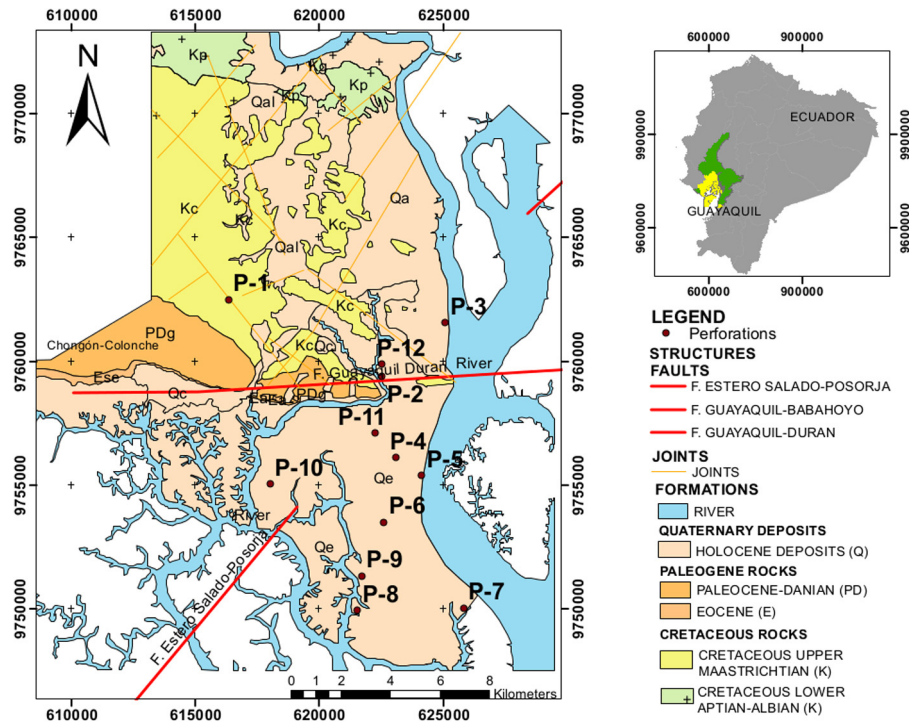
Fig. 1. Geologic map of Guayaquil, Ecuador.

varied the percentage of material, bulk density and moisture content of each type of soil and reported that clay loam soils had lower thermal conductivity than sandy soils. Barry-Macaulay et al. (2013) reported that the thermal conductivity of soil, tested in the laboratory, was influenced by the variation in moisture content, bulk densities, and particle size. This study also highlighted that thermal conductivity of the soil increased with particle size, bulk density, and moisture content. On the other hand, Bovesecchi and Coppa (2013) stated that the degree of consolidation also altered the thermal conductivity of the soil. They reported that consolidated soil showed higher thermal conductivity than their unconsolidated counterpart. Stylianou et al. (2016) analyzed 135 collected samples from 20 geological formations in Cyprus, determining that thermal properties change according to material composition and moisture content. Geological formations containing gypsum presented better thermal properties under dry conditions.

This study is an attempt to propose a geothermic model for the city of Guayaquil and to present suitable sites for efficient geothermal based cooling systems. The model relies on geologic and lithological characterization as well as thermal properties of soil at ten selected sites. There are a few studies in Latin America (Soriano et al., 2015), and this is the first survey of thermal properties of soil carried out in Guayaquil, Ecuador.

2. Methodology

2.1. Geological description of the site

The study area is the center-south of the city of Guayaquil, a part of the Guayas province, as observed in Fig. 1. The geology of this area is related to its geomorphology which consists of three macro-domains, namely: the alluvial plains of Daule and Babahoyo rivers, the deltaic-estuarine soils from the Guayas River and the Chongon-Colonche range.

In chronological order the study areas comprise Holocene deposits of Quaternary (Q), and the sedimentary rocks are from Eocene (E). The alluvial plains (Qa) from the Guayas river are located

in the northeastern part of the city and is associated directly with the flooding plains from the Daule and Babahoyo rivers which form the Guayas River. The deltaic-estuarine complex (Qe) is located in the south-center area of the city composed by the Guayas river and Salado estuary flowing into the sea. The Chongon-Colonche range which belongs to the Cayo formation (P,K), is in the northwestern part of the city and shows a homoclinal structure of average direction N110° constituted by sedimentary rocks from the Cretaceous era.

2.2. Core drilling method and borehole heat exchanger installation

This study is an attempt to map the thermal properties of the soil at ten selected locations to propose a geological-thermal model for city of Guayaquil. Nine drilling sites were located on deltaic-estuary soils and one on rocks of the geological Cayo formation (Ordonez et al., 2006; Benitez et al., 2005). Specifically Table 1 provides the coordinates for each borehole in system UTM-WGS84 with the name of the location and depth of the drilling.

The drilling method was rotopercussion, with recovery of core samples. The drilling equipment was a TP50 core driller mounted on a truck and an ACKER TP-30 on wheels as seen in Fig. 2.

Table 1
Site coordinates (UTM-WGS84) and depth of the ten boreholes.

No.	Location	Depth (m)	Coordinate X	Coordinate Y
P–1	ESPOL	60.00	616350.25	9762495.55
P–2	Univ Guayaquil	60.00	622554.09	9759392.59
P–3	Base Naval Norte	60.00	625099.87	9761545.73
P–4	Centro Civico	50.00	623103.20	9756112.67
P–5	Astinave	50.00	624152.13	9755373.32
P–6	Hospital	60.00	622635.45	9753496.58
P–7	Esclusa	60.00	625843.68	9750023.04
P–8	Base Naval Sur	60.00	621556.55	9749922.25
P–9	Trinitaria	50.00	621732.95	9751321.83
P–10	Suburbio Militar	60.00	618037.44	9755050.60

Fig. 2. Equipment ACKER TP-30 mounted on wheels.

The boreholes were drilled in accordance with the Canadian Standard Association for the design and installation of Energy Systems on Ground (C.S. Association, 2002). The main technical features were the following: depth between 50 m and 60 m, the diameter of the boreholes was 113 mm. The internal diameter of the U-type piping of high-density polyethylene (HDPE) was 19.05 mm, the external diameter was 25.4 mm and the maximum pressure was 723.95 kPa. The space around the U-shaped pipe was filled with a grout of Portland cement and bentonite to improve heat transfer between the pipe and soil as shown in Fig. 3. The thermal response tests were carried out with a GEOCUBE GC700 complying ASHRAE standards (ASHRAE, 2011). These tests consisted of measuring the initial temperature of the soil using water temperature as a proxy, water circulated through the loop at ambient temperature for 20–30 min to reach thermal equilibrium with the ground. Then, the heaters were turned on to increase the water temperature for a minimum period of 48 h to ensure that the system was in a steady state (Kavanaugh, 2000, 2001). During this period the equipment registered the inlet and outlet temperatures every 2 min (see Fig. 3).

The equipment to conduct the thermal response test included a water pump, a series of electric heaters and a data acquisition system to collect flowrate, the inlet and outlet temperature of the water, and power input. The inlet and outlet temperature of the water in the system loop was collected using temperature contact sensors with an uncertainty of ±0.2 °C. The flowrate was also measured with an uncertainty of ±3%. The power provided by the
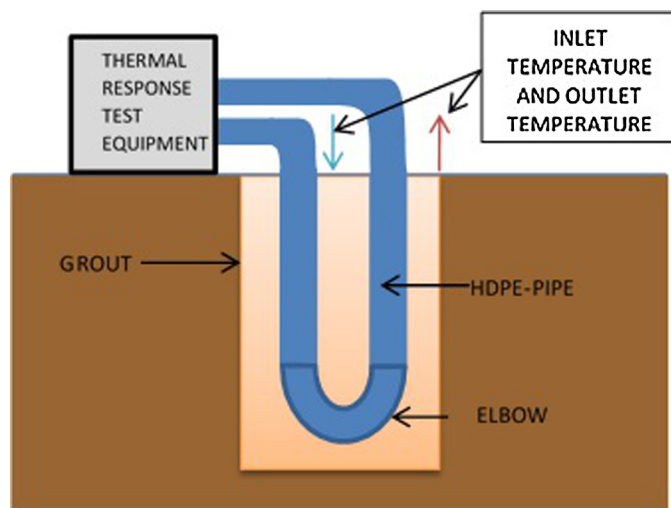

Fig. 3. Schematic of thermal response measurement with GEOCUBE.

electric heaters of water was adjusted to a rate between 50 and 80 W/m through a series of heaters between 2500 and 3000 W. The heating power had an uncertainty of ±3% due to oscillations of the electric generator (Geocube, 2015).

The uncertainty of these in situ measurements was between ±9.6 and ±11.2%. The main factor affecting the precision of these measurements was the testing time (ASHRAE, 2011; Kavanaugh, 2001; Witte et al., 2002).

2.3. Test methods

2.3.1. Sample preparation

Several selected core samples were collected from the drilling process. The specimens were examined to describe the stratigraphic columns based on geotechnical and mineralogical tests. The geotechnical assays performed were humidity determination (UNE, 1993), liquid limit determination (UNE, 1994), plastic limit determination (UNE, 1993), granulometric analysis and solid density (UNE, 1995). The mineralogical analysis was performed using quantitative X-ray diffraction. The results were compared to ASTM standard D 2487-06 and classified according to the unified system of soil classification (ASTM, 2011).

For all samples, a cleaning procedure was carried out to eliminate organic matter, soluble carbonates, and sulfates. The specimens were placed in a flask and washed at least three times with; firstly, hydrogen peroxide to eliminate the organic matter, then a 10% (w/w) hydrochloric acid aqueous solution to remove soluble carbonates, and finally a 30% (w/w) ethylenediaminetetraacetic acid (EDTA) aqueous solution to discard soluble sulfates. During each washing step, the solution of hydrogen peroxide, hydrochloric acid, and EDTA, were extracted using a pipette, then deionized water was added to eliminate any residue. Afterwards, the washed material was allowed to settle for three hours. Finally, the washed samples were placed in an oven at 60 °C for two days. The dried specimen was ground using mortar and pestle and then passed through a 45 μm sieve.

2.3.2. Quantitative X-ray diffraction

After sample preparation, the mineralogical analysis of the core samples was carried out using quantitative X-ray diffraction (QXRD). PANanalytical® X'pert XRD with Kα Cu anode tube using a multi-position detector, X'Celerator®, was utilized. The operating conditions were 40 mA, 45 kV and 0.02° of step size. Additionally, High Score Plus® software was utilized to identify the crystalline phases using the database of International Centre for Diffraction Data (ICDD) and to quantify them using the Inorganic Crystal Structure Database (ICSD). The samples were weighted and 10% (w/w) of zincite was added allowing the quantification of the mineralogical composition and amorphous content. In this regard, a theoretical diffractogram was generated and compared to the experimental diffractogram using Rietveld refinement techniques until reaching at least 5% of the goodness of fit (Bish and Howard, 1988).

2.3.3. Particle size distribution

In this study, two methods of particle size analysis were applied. All samples went through sieve analysis screening test (UNE 103101:95) (UNE, 1995). Sandy samples particle size distribution was also characterized using Megascopic description by a manual stereo microscope and a digital stereo microscope of 1.3 M.

2.3.4. Bulk density

A procedure based on ASTM C20 (ASTM International, 2010) was used to evaluate the density of rock. This procedure, applied to refractory brick and hardened cement pastes, is based on two weight measurements, one in the air and the other under water.

The test procedure used a Metler Toledo® Excellence Plus analytical balance with temperature correction. As the material soaked in ethanol, some wet small pieces were put in a desiccator for a while. The dried samples were weighed. Then, the weighed dry material was placed into a beaker previously filled with distilled water, and another measurement was taken under water after the weight stabilized.

2.4. Thermal properties

Afterwards, the thermal properties of the soil were calculated using the line source analytical method. According to Ingersoll (Ingersoll, 1954), the following must be assumed:

- The heat source had an infinite depth.
- The heat transfer was radial.
- The thermal capacitance of the drilling was small when compared with surroundings and in its interior the temperature variation was negligible.
- The medium should have had a uniform initial temperature.

The ratio of length to diameter of the boreholes, in a range between 440 and 530, made the physical system to approximate closely the first two assumptions. The small diameter of the boreholes (113 mm), when compared with the soil around it made the third assumption an acceptable one. Due to the fact that no thermal sources in the city of Guayaquil have been reported in the literature and considering that in deep layers like the ones the boreholes reached (50 m and 60 m), the temperature distribution remains unchanged and can be considered as almost constant throughout the year (Popiel et al., 2001).

According to Mogensen (1983), the linear model for a vertical drilling is given by Eq. (1) with a diameter (d_b), length (L), heat load ($\dot{Q}$), thermal resistance of the soil (R_s), thermal resistance of the pipe (R_p) and thermal resistance of the circulating fluid (R_f); where ΔT is the difference between the mean temperature of the circulating fluid (T_f) and the unperturbed temperature of the soil (T_g).

$$\Delta T = \frac{\dot{Q}}{4\pi L k_s} \ln t + \frac{\dot{Q}}{L}\left[\frac{\ln\left(16\alpha_s/d_b^2\right) - 0.5772}{4\pi k_s} + R_g + \frac{R_p + R_f}{2}\right] \quad (1)$$

Experimental data could be fitted to Eq. (1) where the slope (m) represents the mean temperature of the coolant (T_b) and the intercept (b) the natural log of the time (ln t). The soil thermal conductivity (k_s) is calculated with the slope and the thermal diffusivity (α_s) with the intercept as shown in Fig. 4 (Mogensen, 1983).

The effective thermal resistance of all U-tubes was calculated using the difference of mean fluid temperature and the temperature of the undisturbed soil divided by the heat load over the height of the borehole as in Eq. (2).

$$R_s(t) = \frac{T_f - T_g}{\frac{\dot{Q}}{L}} \quad (2)$$

In future studies, it will be important to analyze the influence of groundwater flow when its velocities are significantly higher than 0.1 m/day (Signorelli et al., 2007), since the linear model could produce unstable values.

2.5. Thermal model of borehole heat exchanger

The feasibility of using the soil in the city of Guayaquil as a heat sink for cooling applications in buildings is assessed by a thermal model of a borehole heat exchanger. The model analyzes the sensible load dissipated by carrying fluid into the ground and assess
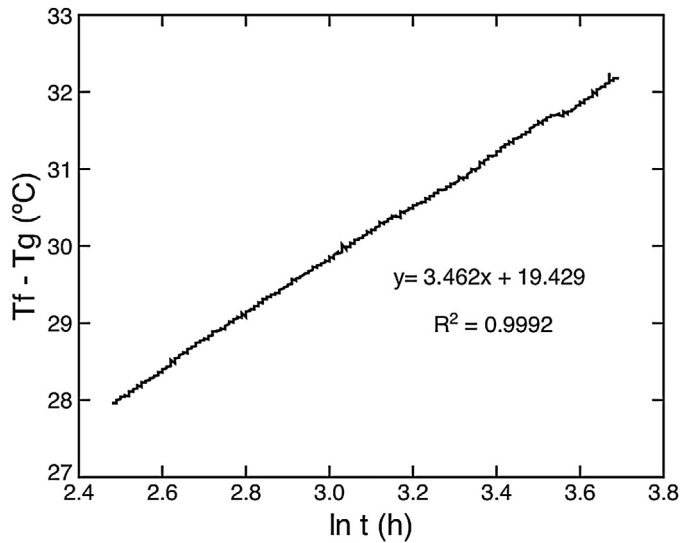

Fig. 4. Linear fit ΔT vs ln(t).

the performance of the heat exchanger under different operating conditions (Soriano and Siguenza, 2015).

The model used in this project is based on TRNSYS software version 17 (Klein, 2010). This software allows building a complete thermal system by means of several modules linked to each other called Types. In our case, the model to represent a borehole heat exchanger is Type 557 which is based on the Duct Ground Heat Storage Model (DST) developed by Hellström (1989). The DST model is focused on the characterization of the temperature profile of the ground around the BHE. This model assumes a cylindrical volume of the ground around the BHE as the storage region, where a 2-dimensional mesh is represented by radial and vertical coordinates. This model calculates the global temperature with the superposition of a global solution, a local solution, and a steady-flux part.

In order to calculate the temperature of the outlet fluid of the BHE a steady-state heat balance is performed as seen in Eq. (3):

$$C_f \dot{m}_f \frac{\partial T}{\partial z} + h(T_f - T_g) = 0 \quad (3)$$

where C_f is the heat capacity of the fluid, $\dot{m}_f$ is the mass flow rate of the circulating fluid, $T_f(z, t)$ is the mean fluid temperature, h is the heat transfer coefficient between the fluid and the surrounding ground with temperature T_g.

The outlet fluid temperature of the BHE can be obtained from Eq. (4) by solving Eq. (3) by integration along the tube (the length coordinate along the flow path is z).

$$T_{f,o} = \beta \ T_{f,i} + (1 - \beta)T_g \quad (4)$$

where $T_{f,o}$ is the outlet temperature, β is a damping factor defined by Eq. (5), and $T_{f,i}$ is the inlet temperature.

$$\beta = \exp\frac{-hL}{C_f \dot{m}_f} \quad (5)$$

It is important to notice that the DST model produces a precise and detailed estimate of the ground temperature evolution of a BHE. Nevertheless, it is based on the steady-state assumption, which could affect the performance of the model for very short time intervals.

3. Results and discussion

3.1. Particle size distribution and mineralogy

In order to provide a general thermal geological model for Guayaquil city, the mineralogical composition and particle size distribution as well as humidity, liquid limit, plastic limit, and bulk density of core samples was examined and related to the thermal respond test. In this study, almost all boreholes showed two big strata. One, from the surface to around 20 m of depth, a multi-band stratum that consists of slit and lignite with different amounts of clayey minerals and sand; another, from around 20 m to 50 m of depth, a sandy layer with different amounts of slit and clayey minerals. The deeper sandy layer is composed of quartz, amphibole, pyroxene, olivine, magnetite, and feldspar observed during megascopic tests. By XRD, the feldspar was identified as anorthite, and clay minerals, nontronite, illite-montmorillonite, and vermiculite.

The deltaic-estuarine complex was studied throughout boreholes P2, P4, P5, P6, P7, P8, P9 and P10 distributed in the center-south of the city as shown in Fig. 1. In the stratigraphic columns, the two strata were easily identifiable: one containing silt, clays, and lignite; the other containing sands. The first strata corresponded to the estuarine soil, in which organic material constitutes the key for identification. The second one that overlaid the first one may pertain to the ancient deposit of the alluvial plains of the Daule River, because of the presence of sands composed of volcanic materials such as amphibole, plagioclase, pyroxene, and quartz.

At rocky sites, P1 and P3 were drilled identifying geological structures belonging to the Cayo formation. This formation is mainly composed of zeolite-rich tuffs up to around 42%; plagioclase, 35%; smectite, 15%. These identified minerals were similar to those reported in the scientific literature (Machiels et al., 2014) for sites near Guayaquil city. P1 was placed within the Chongon Colonche range where lapilli and tuff were mainly observed. P3 was placed in an extension of the deltaic complex of Guayaquil showing similar characteristics to those observed in estuarine deposits.

As the phreatic level is between 0.7 m and 2.0 m in every borehole, except for P1 that is placed in a rocky site, the humidity of the soil in Guayaquil city is about 100%, concluding that these soils are oversaturated.

3.2. Thermal properties

The analysis of thermal properties such as conductivity, diffusivity, and the undisturbed ground temperature was carried out correlating the data obtained from the TRT test and the type of geomorphological-geological units in Guayaquil. Table 2 provides a summary of the results of thermal properties.

Location P1, a rock borehole that corresponds to the Cayo Formation, has the largest thermal conductivity with 1.67 W/m K.

Table 2
Thermal properties summary.

No.	Thermal conductivity (W/m K)	Diffusivity (m²/day)	Undisturbed ground temperature (C)
P-1	1.668	0.378	26.5
P-2	0.898	0.066	28.0
P-3	1.013	0.076	28.5
P-4	1.123	0.012	29.0
P-5	1.245	0.030	29.0
P-6	0.782	0.031	28.0
P-7	0.991	0.038	29.0
P-8	1.120	0.024	28.0
P-10	0.923	0.012	28.0

The deltaic-estuarine complex (sites P2, P3, P4, P5, P6, P7, P8, P9, and P10) exhibits a thermal conductivity in the range of 0.78–1.25 W/m K. The range of thermal diffusivity is between 0.012 and 0.57 m²/day for locations in the deltaic-estuarine complex. The place at the Cayo formation in location P1 has a thermal diffusivity value of 0.38 m²/day. The undisturbed temperature of the soil presents a very narrow range between 26.5 and 29 °C. The values of the ground temperature are between the average maximum and minimum temperature for a typical meteorological year (INAMHI, 2015). Thermal resistivity of the U-loops exhibits a range between 0.34 and 0.57 K/W. The lowest values of thermal resistivity are at locations P4 and P5, corresponding to the two locations with boreholes lengths of 50 m.

The measurements done in Guayaquil show that the temperature of the soil is between 27 and 29 °C (Soriano and Villanueva, 2015). This temperature is significant when compared to the 22 °C found in the southern part of US, 21 °C in Dubai or 17.5 °C in Algeria (Lund et al., 2004). The values surveyed are similar to those found at more tropical locations such as Saudi Arabia (32 °C) and Nigeria (32.5 °C) (Sharqawy et al., 2009; Oladunjoye and Sanuade, 2012), complicating the heat transfer to the soil and reducing the efficiency of GSHPs. With respect to thermal conductivity values are between 0.782 and 1.668 W/m K, which is within the range of previous values of 1.3 W/m K in Algeria (Sharqawy et al., 2009) and 1.7 W/m K in Chile (Roth et al., 2004), suitable for thermal dissipation in the soil with the best location at the Cayo Formation.

3.3. Litho-stratographic profile

With the particle size distribution and mineralogy data, the stratigraphic profile was built. The stratigraphic profile describes the predominant soils in the deltaic-estuarine deposit as seen in Fig. 5.

From surface to bottom, the soil in Guayaquil has approximately 8 m of fill dirt varying with location. A silt strata with a depth of 20–25 m follows the fill dirt; these strata have silt with high-low plasticity and discontinuities of high plasticity clay of up to 9 m, lignite of up to 5 m and silty sand of up to 5 m. At most locations, the silt is composed of an interlayer of fine and coarse sand. Additionally, it contains large amounts of organic materials such as branches, leaves, and shells. In some zones, acicular minerals such as gypsum and sulfur are present. Also, there are large amounts of clay and silt nodules showing oxidation signs; at location P9, a large quantity of reddish silt was observed. The low plasticity silt contains plagioclase type anorthite, quartz and smectite type nontronite. The high plasticity clay and lignite consist of plagioclase type anorthite, quartz, illite-montmorillonite and vermiculite mica.

Below the silt strata there is one of poorly graded silty sand, in some locations with depths of up to 30 m. The sand strata have minerals such as quartz, anorthite type feldspar, amphiboles, olivines, and pyroxenes. Smaller percentages of magnetite, limestone, mica, and pyrite were also identified. In the Deltaic complex – location P3 Base Naval Norte – at the same level of the sand strata, a volcanoclastic rock lapilli type from the Cayo Formation was found.

The next 30 m consisted of two strata, one of clay overlaying and one of sand. These strata were characterized with the help of reference columns.

3.4. Geological-thermal map

The nomenclature of the geological map was taken from the Stratigraphic Chart (Ogg, 2009), and from other studies carried out in the city of Guayaquil (Benitez et al., 2005; Ordonez et al., 2006). The maps of thermal conductivity (Fig. 6), thermal diffusivity (Fig. 7), and undisturbed ground temperature (Fig. 8) were built with the software QGis. The maps were built using the
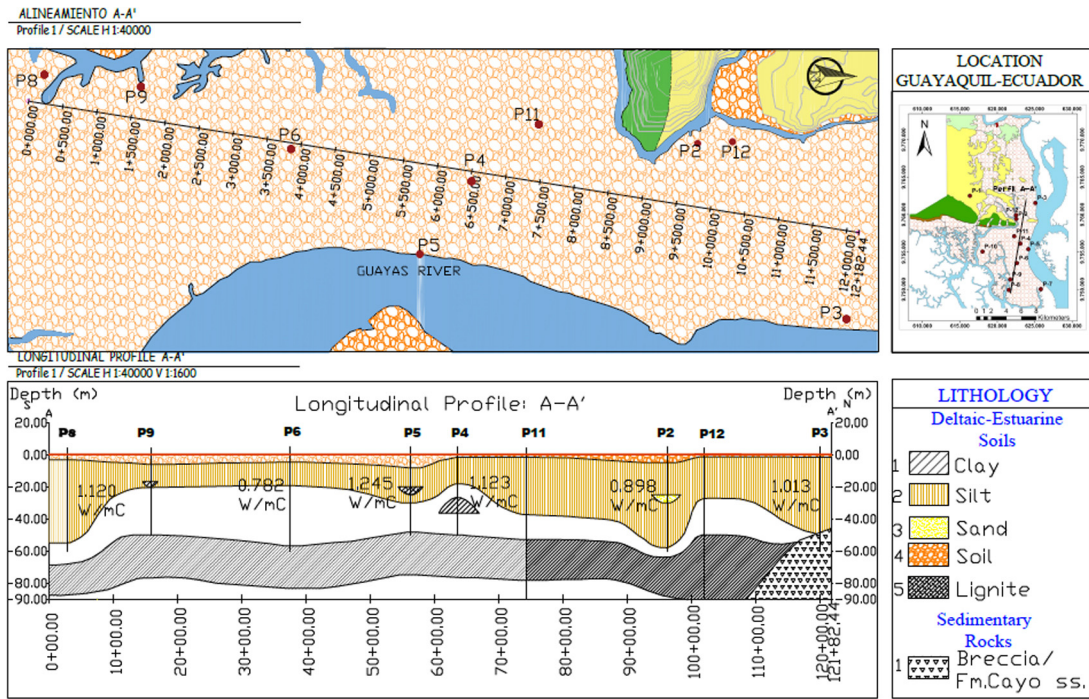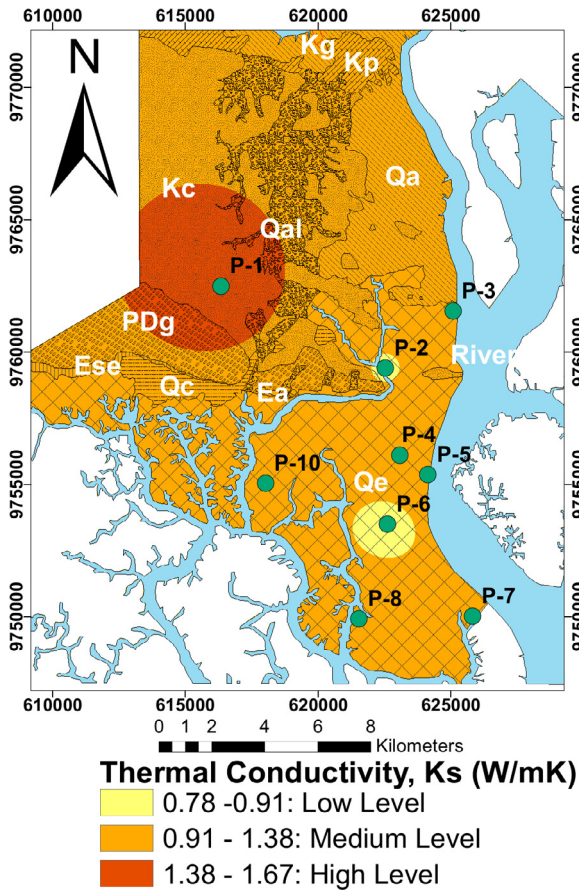
Fig. 5. Stratigraphic profile.
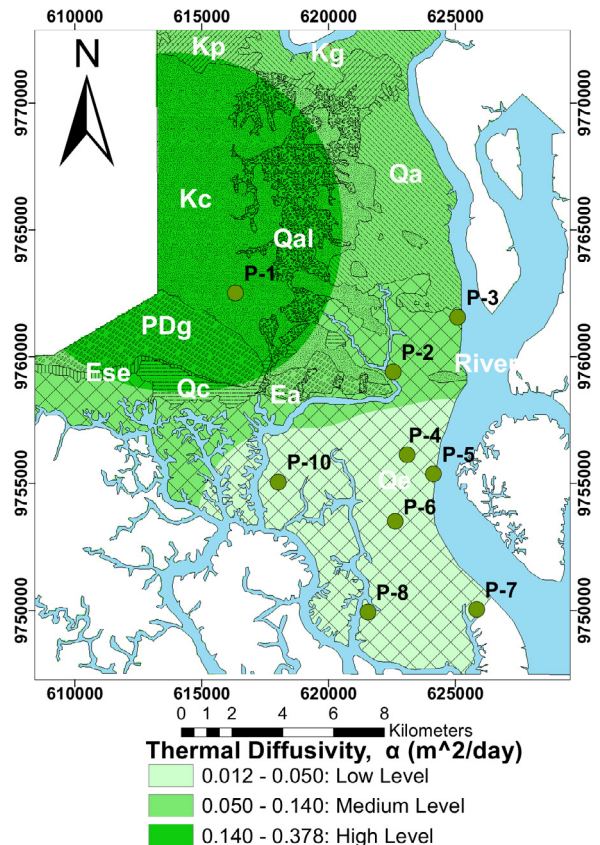

Fig. 6. Thermal conductivity map.

Fig. 7. Thermal diffusivity map.

Undisturbed Temperature, To (°C)

26.50 - 27.75: Low Level

27.75 - 28.45: Medium Level

28.45 - 29.00: High Level

Fig. 8. Average undisturbed ground temperate map.

Table 3
Physical borehole parameters.

Parameter	Symbol [unit]	Value
Borehole and homogeneous material		
Depth	H [m]	50
Diameter	D [m]	12
Pipe (HDPE)		
Internal diameter	d_i [mm]	20.07
External diameter	d_o [mm]	25.4
Roughness	e [mm]	0.0015
Distance between centres	a [mm]	70
Thermal conductivity	k [W/m K]	0.44

Table 4
Thermal model results.

No.	Heat dissipation – steady state (W/m)
P-1	30.0
P-2	13.1
P-3	16.0
P-4	16.4
P-5	19.3
P-6	13.7
P-7	15.9
P-8	16.8
P-10	13.4

inverse distance method (IDW) (Shepard, 1968)to perform the interpolation in the influence radius of the sampled value.

In the maps, the geology is also plotted overlapping the thermal properties like thermal conductivity, thermal diffusivity and undisturbed ground temperature.

As a result, the highest values of thermal conductivity are observed in breccia, lapilli, and volcanic tuffs from the Cayo Formation. The deltaic-estuarine soils are on the high range, except P6. In the case of thermal diffusivity, very high values in the rocky area i.e. P1 are observed, and the complex deltaic-estuarine that shows a medium range, apart from P2 and P3 that are high. The undisturbed ground temperature exhibits higher values in the southern parts of the city placed in the complex deltaic-estuarine where tides and water circulation meaningfully affect these locations.

It seems that P1 shows the best thermal properties because it is a rocky content. In the complex deltaic-estuarine, the conductivity is better in the Astinave location, while Centro Civico, Suburbio Militar, Esclusas, Base Naval Sur and Base Naval Norte present lower values. Besides, for thermal diffusivity it is observed that it is higher in the northern locations when compared with locations in center-south.

3.5. Thermal model simulation

The borehole heat exchanger (BHE) performance was simulated using TRNSYS 17 (Klein, 2010). In the software, a compilation of components created a closed loop system along the BHE using water as the heat transfer fluid. The system included the following;

firstly, Guayaquil's weather data component Type 15-6 as well as a simple ground temperature model Type 77. Also, the main component Type 557a that represents the vertical "U" type vertical heat exchanger. Finally, a Type 6 auxiliary heater component in addition to a single speed pump with no power coefficients Type 3d and two online plotter with supplied units. The model was set to run for 10,000 h of operation.

The homogeneous material properties such as the thermal conductivity, density and heat capacity were considered to be the same as the estuarine ground found in Table 2. This condition is assumed due to the relatively high volume ratio between the ground and the grouting. Additionally, the flowrate was set to 1×10^{-4} m^3/s and the inlet temperature to 45 °C which are considered typical values in real ground source heat systems. The main borehole model parameters are presented in Table 3.

3.5.1. Results of thermal model

Table 4 shows results of the heat transfer simulation for a single borehole at each of the conditions measured in Guayaquil. The main result is the capacity of a single borehole to dissipate heat into the ground under continuous operation once it reaches steady state. In other words, the capacity of the soil to act as a heat sink is reported.

Results show capacities between 13 and 30 W/m under steady state and continuous operation. The maximum performance is in the perforation located at ESPOL which is part of the Cayo geological formation in Guayaquil. Lower dissipation rates are achieved in the deltaic-estuarine soil with the point at University of Guayaquil having the lowest performance.

It is worth mentioning that peak dissipation rates above 50 W/m are possible for short periods as demonstrated by conditions imposed in the thermal response tests at every site.

4. Conclusions

The first study of thermal properties in Guayaquil, Ecuador is presented. The study constitutes one of the first in this region of the world. The study was carried out through nine boreholes in the deltaic-estuarine deposits and one borehole the Cayo Formation which is a rocky deposit. The range of the borehole depth was between 40 m and 60 m.

In the stratigraphic profile of the deltaic-estuarine deposit, it is possible to recognize two strata, one of silt with inserts of clay and lignite that has between 20 and 25 m in depth; and other of sand with clay and silt nodules with approximately 30 m of depth. The phreatic level at this area was between 0.7 m and 2 m. The Cayo formation was constituted by sedimentary rocks, but no phreatic level was found at this location.

The results of the TRTs showed two very distinct behaviors in thermal properties between the deltaic-Estuarine zone and the Cayo formation. The geological unit of the deltaic-estuarine complex showed values of thermal conductivity between 0.782 and 1.245 W/m K which are lower than that of the rocky place (i.e., 1.668 W/m K). In addition, the phreatic level between 0.7 m and 2 m and mineralogical composition affected such values of thermal conductivity in the deltaic-estuarine zone but not enough to reach the levels of the Cayo Formation. All measurements were similar to those reported by other authors at similar geological regions.

The values of the temperature of the soil are within the range of previous reported values for locations at a similar latitude. Typical temperature gradients between soil and average ambient temperature in Guayaquil are below 5 °C. These temperature gradients are not adequate for traditional direct cooling applications of buildings. However, thermal load dissipation of a building is possible.

The thermal model showed that an individual borehole heat exchanger can dissipate between 10 and 30 W/m when reaching steady state with typical operating conditions of inlet temperatures of 45 °C and flowrates of 1×10^{-4} m^3/s. The decision of using ground as a final heat sink of HVAC systems should be based on a case by case technical and economical analysis and further studies are required.

The maps should be a framework for coming engineering projects contributing to decision-making process related to HVAC systems. In the case of Guayaquil-Ecuador, this study is a starting point to develop more efficient geothermal based cooling systems.

Acknowledgment

References

Abu-Hamdeh, N., Khdair, A., Reeder, R., 2001. A comparison of two methods used to evaluate thermal conductivity for some soils. Int. J. Heat Mass Transf. 44 (5), 1073–1078.

Aldossary, N., Rezgui, Y., Kwan, A., 2014. Domestic energy consumption patterns in a hot and humid climate: a multiple-case study analysis. Appl. Energy 114, 353–365.

Anand, S., Gupta, A., Tyagi, S., 2014. Solar cooling systems for climate change mitigation: a review. Renew. Sustain. Energy Rev. 41, 143–161.

ASHRAE, 2011. Chapter 34: Geothermal Energy, 2011 ASHRAE HANDBOOK – HVAC Applications. ASHRAE, Atlanta, GA, pp. 34.1–34.34.

ASTM International, 2010. Test Methods for Apparent Porosity, Water Absorption, Apparent Specific Gravity, and Bulk Density of Burned Refractory Brick and Shapes by Boiling Water. ASTM International.

UNE, 2011. Practice for Classification of Soils for Engineering Purposes (Unified Soil Classification System). ASTM International.

Banjac, M., Todorović, M., Ristanović, M., Galić, R., 2012. Experimental determination of thermal conductivity of soil with a thermal response test. Therm. Sci. 16 (4), 1117–1126.

Barry-Macaulay, D., Bouazza, A., Singh, R., Wang, B., Ranjith, P., 2013. Thermal conductivity of soils and rocks from the Melbourne (Australia) region. Eng. Geol. 164, 131–138.

Benitez, S., Alvarez, V., Vera, X., Mera, W., 2005. Investigacion y estudio del comportamiento dinamico del subsuelo y microzonificacion sismica de la ciudad de Guayaquil. Geological study, Universidad Catolica de Guayaquil.

Best, R., Rivera, W., 2015. A review of thermal cooling systems. Appl. Therm. Eng. 75, 1162–1175.

Bish, D.L., Howard, S.A., 1988. Quantitative phase analysis using the Rietveld method. J. Appl. Crystallogr. 21 (2), 86–91.

Boukli Hacene, M., Amara, S., Chabane Sari, N., 2012. Analysis of the first thermal response test in Algeria. J. Therm. Anal. Calorim. 107, 1363–1369.

Bovesecchi, G., Coppa, P., 2013. Basic problems in thermal-conductivity measurements of soils. Int. J. Thermophys. 34 (10), 1962–1974.

C.S. Association, 2002. Design and installation of earth energy systems, Standard C448-02. CSA, Rexdale, ON.

Chan, H.-Y., Riffat, S., Zhu, J., 2010. Review of passive solar heating and cooling technologies. Renew. Sustain. Energy Rev. 14 (2), 781–789.

De Vries, D.A., 1963. Thermal properties of soils. In: Physics of Plant environment.

El-Dessouky, H., Ettouney, H., Al-Zeefari, A., 2004. Performance analysis of two-stage evaporative coolers. Chem. Eng. J. 102 (3), 255–266.

Esen, H., Inalli, M., 2009. In-situ thermal response test for ground source heat pump system in Elaziğ, Turkey. Energy and Buildings 41, 395–401.

Florides, G., Kalogirou, S., 2007. Ground heat exchangers – review of systems, models and applications. Renew. Energy 32 (15), 2461–2478.

Fong, K., Chow, T., Lee, C., Lin, Z., Chan, L., 2010. Comparative study of different solar cooling systems for buildings in subtropical city. Sol. Energy 84 (2), 227–244.

Geocube, 2015. Precision Geothermal LLC, Maple Plain, User's manual for geocube.

Hellström, G., 1989. Duct ground heat storage model, manual for computer code. Department of Mathematical Physics, University of Lund, Sweden.

INAMHI, 2015. Weather Yearbook 2015 (Ecuador). Tech. rep. INAMHI.

Ingersoll, L.R., 1954. Heat Conduction; With Engineering, Geological, and Other Applications. University of Wiscons, Madison, iD: 00936186.

Johansen, O., 1977. Thermal conductivity of soils, Tech. rep. DTIC Document.

Kasubuchi, T., 1984. Heat conduction model of saturated soil and estimation of thermal conductivity of soil solid phase. Soil Sci. 138 (3), 240–247.

Kavanaugh, S.P., 2000. Field tests for ground thermal properties – methods and impact on ground-source heat pump design. In: ASHRAE. (Ed.), In: ASHRAE Transactions, vol. 106, pp. 851–855.

Kavanaugh, S.P., XL, MC, 2001. Investigation of methods for determining soil and rock formation thermal properties from short-term field tests, Technical 1118-TRP. ASHRAE.

Kharseh, M., Al-Khawaja, M., Suleiman, M., 2015. Potential of ground source heat pump systems in cooling-dominated environments: residential buildings. Geothermics 57, 104–110.

Klein, S.A., 2010. University of Wisconsin-Madison. Solar Energy Laboratory, TRNSYS 17, a transient system simulation program, Solar Energy Laboratory. University of Wisconsin-Madison.

Lu, S., Wei, S., Zhang, K., Kong, X., Wu, W., 2013. Investigation and analysis on the energy consumption of starred hotel buildings in Hainan Province, the tropical region of China. Energy Convers. Manage. 75, 570–580.

Lund, J., Sanner, B., Rybach, L., Curtis, R., Hellström, G., 2004. Geothermal (ground-source) heat pumps – a world overview. GHC Bull. 25 (3), 1–10.

Machiels, L., Garcés, D., Snellings, R., Vilema, W., Morante, F., Paredes, C., Elsen, J., 2014. Zeolite occurrence and genesis in the late-cretaceous Cayo arc of coastal Ecuador: evidence for zeolite formation in cooling marine pyroclastic flow deposits. Appl. Clay Sci. 87, 108–119.

Mogensen, P., 1983. Fluid to duct wall heat transfer in duct system heat storages. In: Document – Swedish Council for Building Research., pp. 652–657.

Ogg, G., 2009. International stratigraphic chart. International Commission on Stratigraphy.

Oladunjoye, M.A., Sanuade, O.A., 2012. In situ determination of thermal resistivity of soil: case study of Olorunsogo power plant, southwestern Nigeria. ISRN Civil Engineering.

Ordonez, M., Jimenez, N., Suarez, J., 2006. Micropaleontologia ecuatoriana, Petroproduccion and Centro de Investigaciones Geologicas, Guayaquil, Ecuador (in Spanish).

Pintaldi, S.B., Perfumo, C., Sethuvenkatraman, S., White, S., Rosengarten, G., 2015. A review of thermal energy storage technologies and control approaches for solar cooling. Renew. Sustain. Energy Rev. 41 (1), 975–995.

Popiel, C.O., Wojtkowiak, J., Biernacka, B., 2001. Measurements of temperature distribution in ground. Exp. Therm. Fluid Sci. 25 (5), 301–309.

Roth, P., Georgiev, A., Busso, A., Barraza, E., 2004. First in situ determination of ground and borehole thermal properties in Latin America. Renew. Energy 29 (12), 1947–1963.

Ruiz-Calvo, F., Montagud, C., 2014. Reference data sets for validating gshp system models and analyzing performance parameters based on a five-year operation period. Geothermics 51, 417–428.

Sanner, B., Karytsas, C., Mendrinos, D., Rybach, L., 2003. Current status of ground source heat pumps and underground thermal energy storage in Europe. Geothermics 32 (4–6), 579–588, Selected Papers from the European Geothermal Conference 2003.

Sharqawy, M.H., Said, S., Mokheimer, E., Habib, M., Badr, H., Al-Shayea, N., 2009. First in situ determination of the ground thermal conductivity for boreholeheat exchanger applications in Saudi Arabia. Renew. Energy 34 (10), 2218–2223.

Shepard, D.,1968. A two-dimensional interpolation function for irregularly-spaced data. In: Proceedings of the 1968 23rd ACM National Conference. ACM, pp. 517–524.

Shim, B., Park, C.-H., 2013. Ground thermal conductivity for (ground source heat pumps) GSHPs in Korea. Energy 56, 167–174.

Signorelli, S., Bassetti, S., Pahud, D., Kohl, T., 2007. Numerical evaluation of thermal response tests. Geothermics 36 (2), 141–166.

Soriano, G., Siguenza, D., 2015. Thermal performance of a borehole heat exchanger located in Guayaquil – Ecuador using novel heat transfer fluids. In: ASME 2015

International Mechanical Engineering Congress and Exposition, American Society of Mechanical Engineers, pp. V06AT07A054–V06AT07A054.

Soriano, G., Villanueva, R., 2015. Technical report of energy use comparison between a cooling tower and ground source heat exchange at base naval sur Guayaquil, Tech. rep. INER, Quito, Ecuador.

Soriano, G., Villanueva, R., Gonzalez, I., Lopez, K., Cornejo, M., 2015. First in situ measurement of soil thermal response in Guayaquil, Ecuador. Energy Sustain. VI 195, 327.

Stylianou, I.I., Tassou, S., Christodoulides, P., Panayides, I., Florides, G., 2016. Measurement and analysis of thermal properties of rocks for the compilation of geothermal maps of Cyprus. Renew. Energy 88, 418–429.

Tsai, J.-H., Wu, C.-P., Chang, H.-C., 2014. An investigation of geothermal energy applications and assisted air-conditioning system for energy conservation analysis. Geothermics 50, 220–226.

UNE, 1993. Test for Plastic Limit of Soil, UNE 103104:93. UNE.

UNE, 1993. Test Method for Determination of Water (Moisture) Content of Soil by Microwave Oven Heating, UNE 103300:93. UNE.

UNE, 1994. Determination of the liquid limit of a soil by the casagrande apparatus method, UNE 103103:94. UNE.

UNE, 1995. Particle Size Analysis of a Soil by Screening, UNE 103101:95. UNE.

Witte, H., Gelder, A., Van Spitler, J., 2002. In-situ measurement of ground thermal conductivity: the Dutch perspective. ASHRAE Trans. 108 (1).

Yau, Y., Hasbi, S., 2013. A review of climate change impacts on commercial buildings and their technical services in the tropics. Renew. Sustain. Energy Rev. 18, 430–441.

Zeyghami, M., Goswami, D., Stefanakos, E., 2015. A review of solar thermo-mechanical refrigeration and cooling methods. Renew. Sustain. Energy Rev. 51, 1428–1445.